ARTICLE

OBC
www.rsc.org/obc

Ab initio MO study on [3 + 2] annulation using β-phenylthio-acryloylsilanes with alkyl methyl ketone enolates and its through-space/bond interaction analysis

Yuuichi Orimoto,[a] Kazunari Naka,[b] Kei Takeda[c] and Yuriko Aoki*[d,e]

[a] *Department of Molecular and Material Sciences, Interdisciplinary Graduate School of Engineering Sciences, Kyushu University, 6-1 Kasuga Park, Fukuoka, 816-8580, Japan*

[b] *Department of Chemistry, Graduate School of Science, Hiroshima University, 1-3-1 Kagamiyama, Higashi-Hiroshima, 739-8526, Japan*

[c] *Department of Synthetic Organic Chemistry, Graduate School of Medical Sciences, Hiroshima University, 1-2-3 Kasumi, Minami-ku, Hiroshima, 734-8551, Japan*

[d] *Department of Molecular and Material Sciences, Interdisciplinary Graduate School of Engineering Sciences, Kyushu University, 6-1 Kasuga Park, Fukuoka, 816-8580, Japan. E-mail: aoki@cube.kyushu-u.ac.jp; Fax: +81-92-583-8834; Tel: +81-92-583-8834*

[e] *Group, PRESTO, Japan Science and Technology Agency (JST), Kawaguchi Center Building, 4-1-8 Honcho, Kawaguchi, Saitama, 332-0012, Japan*

Received 9th March 2005, Accepted 26th April 2005
First published as an Advance Article on the web 13th May 2005

Ab initio through-space/bond interaction analysis was applied to [3 + 2] annulation based on Brook rearrangement using β-phenylthio-acryloylsilanes with alkyl methyl ketone enolates. An uncertain reaction mechanism, wherein a bulky cyclopentenol with large substituents on the same side of the five-membered ring was obtained as a major product, can be explained by the low activation energy of its reaction pathway. Intramolecular orbital interactions related to the carbanion generated by Brook rearrangement preferentially provide the stabilization of the reaction pathway to the bulky cyclopentenol (major product) compared with that provided to the non-bulky cyclopentenol (minor product). In addition, *ab initio* molecular orbital calculations suggest the existence of an *E*/*Z* conformational inversion after Brook rearrangement. This result accurately explains the loss of the *E*/*Z* stereochemical integrity in the starting materials of the experiment.

Introduction

Techniques for the production of five-membered carbocycles have created considerable interest in recent years because cyclopentane rings are involved in the production of important medical supplies and natural products. Several investigations have been made on the annulation techniques used for preparing five-membered carbocycles.[1] The [3 + 2] annulation technique[2] is an important method for performing stereoselective constructions of cyclopentane rings with substituent groups. One of the authors, Takeda *et al.*, proposed a new method[3–6] to synthesize cyclopentenol derivatives using a [3 + 2] annulation treatment based on Brook rearrangement.[7] Its synthetic utility was underscored by the composition of several natural products.[8]

Scheme 1 illustrates the [3 + 2] annulation based on Brook rearrangement using β-phenylthio-acryloylsilanes **1** with alkyl methyl ketone enolates **2**. The [3 + 2] annulation using R = Et[3] was conducted under heating from −80 °C to −30 °C, with lithium diisopropylamide (LDA) in tetrahydrofuran (THF) solution. A mixture of *E*/*Z* isomers **1** provided cyclopentenols **3** (yield 70%, major product) and **4** (5%, minor product), although the cyclopentenol **3** is bulkier than is **4** due to steric repulsion between the phenylthio and ethyl groups. In addition, it was reported that the *E*/*Z* ratio of starting material **1** does not affect the ratio of cyclopentenols **3** to **4**. For comparison, [3 + 2] annulation using R = Me[6] was performed under a variety of conditions. A highly purified (*E*)-**1** afforded **3** (68%) and **4** (2%) after being heated from −80 °C to −30 °C, with LDA in THF solution. Similarly, purified (*Z*)-**1** afforded **3** (73%) and **4** (5%) under the same conditions. It was also reported that purified (*E*)-**1** leads to *E*/*Z* isomerization ((*E*)-**1** : (*Z*)-**1** = 1 : 1.4) after 10 min at −80 °C without heating. Takeda *et al.* presumed that the *E*/*Z* isomerization is caused by an *E*/*Z* conformational inversion. Scheme 2 (R′$_3$ = Me$_2$Bu^t) shows the expected reaction pathway from (*E*)-**1** to (*Z*)-**1**. The reaction of (*E*)-**1** with **2** provides (*E*)-**5** and Brook rearrangement in (*E*)-**5** leads to (*E*)-**6**, including delocalized allylic anions. These steps are reversible processes. The delocalization of a negative charge in the carbanion weakens the olefin's double bond between $C_{(B)}$ and $C_{(C)}$, thus facilitating the *E*/*Z* conformational inversion. Because the distinction between (*E*)-**6** and (*Z*)-**6** disappears due to the *E*/*Z* inversion, it is expected that experimental results would not be affected by the stereochemistry of the starting materials. The last irreversible step, including intramolecular cyclization ((*E*)-**6** → **3** and **4**), is caused by the attacking of the negative charge on $C_{(B)}$ to $C_{(H)}$ of the carbonyl group.

There are several uncertain points in this projected reaction pathway. (1) Cyclopentenol **3** seems to have a disadvantage for reactivity in the last cyclization step compared with **4** because of the large repulsion between the substituent groups. Therefore, why does the bulkier **3** become the major product? (2) In a previous paper,[6] Takeda *et al.* suggested that *E*/*Z* isomerization was caused by *E*/*Z* inversion even at low temperatures. However, *E*/*Z* inversion has not yet been proved either experimentally or theoretically.

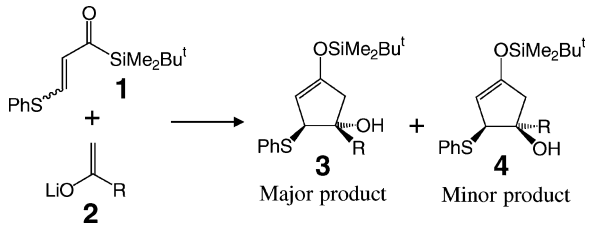

Scheme 1

DOI: 10.1039/b503520a

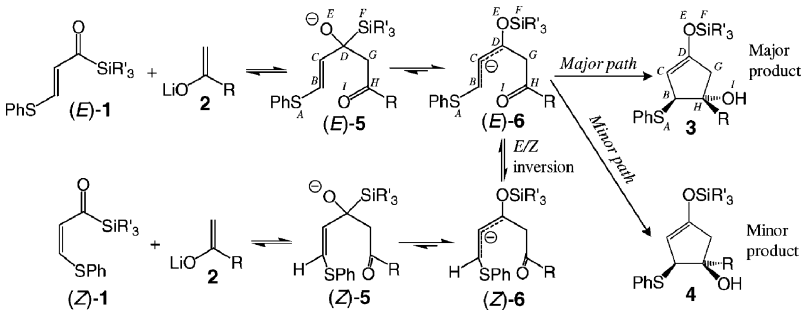

Scheme 2

The concept of through-space/bond interactions was originally proposed by Hoffmann *et al.* in 1968[9] and has been applied in various fields of chemistry.[10] The concept divides the numerous types of intramolecular interactions into only two types; that is, interactions through space and through bond. *Ab initio* through-space/bond interaction analysis[11] was developed to elucidate the stereoelectronic effects[12] in organic compounds by quantitatively estimating the specific orbital interactions in a molecule. This treatment was improved by including the effects of electron correlations, and it was applied to rotational barriers,[13] conjugation effects[14] and so on.

In the present paper, we perform *ab initio* through-space/bond interaction analysis to elucidate the uncertain reaction mechanisms of the [3 + 2] annulations. It was found that the orbital interactions related to carbanion are the cause of the difference in the stability of transition states between in (*E*)-**6** → **3** and in (*E*)-**6** → **4**. This effect supports the experimental result that the bulky cyclopentenol **3** is obtained as a major product. In addition, *ab initio* molecular orbital (MO) calculations showed that the rotational barrier from (*E*)-**6** to (*Z*)-**6** is smaller than the activation energy of the cyclization steps. This implies that *E*/*Z* isomerization can occur due to the *E*/*Z* inversion in the delocalized allylic anion in (*E*)-**6**.

Methods

In *ab initio* through-space/bond interaction analysis, we can quantitatively estimate the contribution of specific orbital interactions to the whole molecule in terms of the deletion of the interactions by modifying the exponents in the basis functions that correspond to the interactions. We consider the estimation of the interaction between atomic orbitals (AOs) χ_r and χ_s, which belong to different atoms, respectively. For the off-diagonal elements of AO integrals corresponding to the interaction, we use artificial AO integrals obtained by contracted basis functions. In the contracted basis functions, the absolute magnitude of the exponents in the Gaussian-type functions gradually increases to an extremely large value. When the exponents have such large values, the two orbitals, χ_r and χ_s, are completely localized on each nucleus. All the off-diagonal elements of the AO integrals corresponding to the interaction lead to zero because the orbital overlap between χ_r and χ_s becomes zero (refer to Ref. 11).

The procedures for the *ab initio* through-space/bond interaction analysis are summarized in the following paragraphs (see Fig. 1).

(1) Normal AO integrals are calculated by using normal AO basis functions and artificial AO integrals are calculated by using artificially contracted AO basis functions with large exponents. Normal and artificial AO integrals are stored in file-1 and file-2, respectively.

(2) AO integrals corresponding to the interactions that we want to delete are extracted from file-2 (large exponent). Other integrals corresponding to the interactions that we want to retain are extracted from file-1 (normal exponent). This "merging" process provides a new file of AO integrals for the through-space/bond interaction analysis.

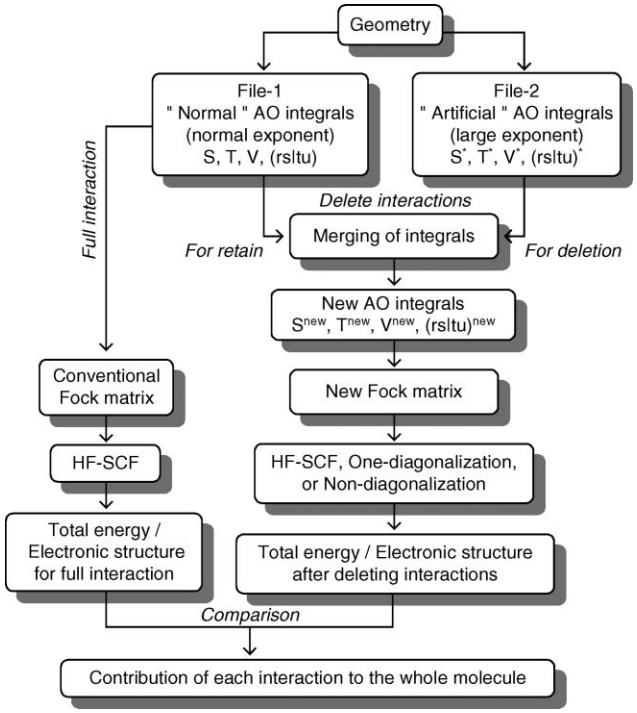

Fig. 1 Flowchart of the procedures for *ab initio* through-space/bond interaction analysis. *S*, *T*, *V* and (*rs*|*tu*) indicate overlap integral, kinetic energy integral, nucleus-electron attractive integral and two-electron integral, respectively.

(3) A new Fock matrix for the through-space/bond analysis is composed of the new AO integrals file obtained by the "merging" process. Conventional Hartree–Fock self-consistent field (HF-SCF) treatment using the new Fock matrix provides us with the total energy and electronic structure of the molecule after deleting the specific orbital interactions. In this step, we can select other treatments; for example, a process that includes only one diagonalization of the Fock matrix, a process that includes only a calculation of total energy (without diagonalization) and so on. The one-diagonalization process was adopted throughout this work.

These procedures are incorporated into the GAMESS program package.[15]

In the present article, the through-space/bond interaction analysis was performed using the HF/6-31G basis set. Because the direct SCF treatment had not been incorporated into the analysis, a basis set larger than HF/6-31G was not used in the present calculations. We deleted the through-space interactions between the "outer" orbitals of the split valence p-type functions (p^{outer}) throughout this work because the contribution of the large orbitals is important for through-space interactions. For

example, if we want to delete the through-space interactions between a sulfur atom and an oxygen atom, all the combinations of the $3p^{outer}_{(x,y,z)}$ orbitals (belonging to the sulfur atom) and the $2p^{outer}_{(x,y,z)}$ orbitals (belonging to the oxygen atom) should be deleted. Except for the through-space/bond analysis, *ab initio* MO calculations were performed using the Gaussian98 program package.[16]

Model molecules

In this work, we considered the reaction pathway related to the (*E*)-isomer with R = Et in the [3 + 2] annulation, as shown in Scheme 2. For the first step of the analysis, we adopted several approximations: (i) the bulky substituent $R'_3 = Me_2Bu^t$ was replaced with $R'_3 = H_3$. (ii) The Li^+ atom in the solution was not considered. (iii) We neglected stabilization of the ion molecules by solvation effects because of the small permittivity of THF solution ($\varepsilon = 7.58$) compared with that of water ($\varepsilon = 78.39$). Major and minor pathways are defined as the reaction pathways leading to the major and minor products in the cyclization step, respectively.

Results and discussion

Comparison of activation energies of major and minor pathways in cyclization step

First, we examined the activation energies for the major and minor pathways in the cyclization step of [3 + 2] annulation. The activation energy $\Delta E^{\ddagger}$ is defined as the difference in total energy between the transition state (TS) and the reactant (REAC), that is, $\Delta E^{\ddagger} = E_{total}{}^{TS} - E_{total}{}^{REAC}$. The geometry of TS was optimized for both the major and minor pathways (HF/6-31G). The geometries of REAC and the product (PROD) were obtained by the intrinsic reaction coordinate (IRC) method[17] using the same basis set. Fig. 2 illustrates the optimized geometries for the major ((*E*)-**6** → **3′**) and minor ((*E*)-**6** → **4′**) pathways, where the prime sign of **3′** and **4′** denotes the molecules before protonation. The total energy changes (HF/6-31G) for these reaction pathways are shown in Fig. 3. Although the geometry of REAC was slightly different between the major and minor pathways, as shown in Fig. 2, their total energies were nearly equal. In REAC, the carbonyl groups in both pathways rotate about the $C_{(G)}$–$C_{(H)}$ bond (see Scheme 2) in opposite directions from each other towards TS. The activation energy $\Delta E^{\ddagger}$ was estimated with 13.37 kcal mol^{-1} for the major pathway and 15.85 kcal mol^{-1} for the minor pathway. This means that the major pathway in the cyclization step has a lower activation energy $\Delta E^{\ddagger}$ than the minor pathway by 2.48 kcal mol^{-1}. We also conducted geometry optimizations for the same reaction pathways at the level of HF/6-31G(d). In this level of calculations, $\Delta E^{\ddagger}$ was estimated with 15.97 and 17.06 kcal mol^{-1} for the major and minor pathways, respectively, and the $\Delta E^{\ddagger}$ of the major pathway was lower than that of the minor pathway by 1.09 kcal mol^{-1}. These results showed a tendency similar to the HF/6-31G results. The lower activation energy of the major pathway reproduces the experimental result that bulky cyclopentenol **3** becomes a major product. However, an unsettled question remains: "what makes the difference in activation energies between the major and minor pathways?" We will discuss this question in the next section.

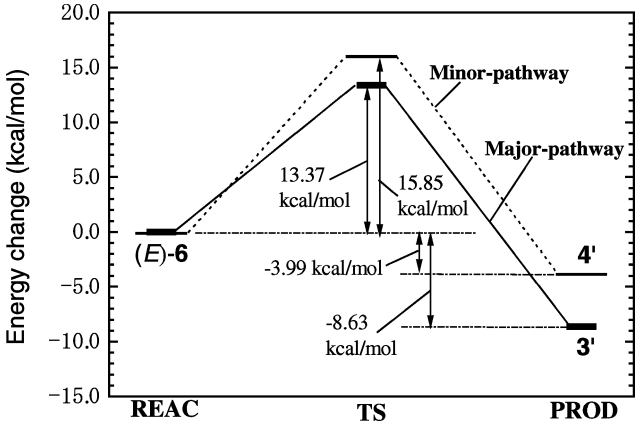

Fig. 3 Total energy changes (in kcal mol^{-1}) for major ((*E*)-**6** → **3′**, thick bar connected by solid line) and minor ((*E*)-**6** → **4′**, thin bar connected by dotted line) pathways in the cyclization step (HF/6-31G). Relative energies compared with the total energy of (*E*)-**6** in the major pathway are plotted on the graph.

In PROD, the total energy of **3′** is lower than that of **4′** by 4.65 kcal mol^{-1}, as opposed to the prediction that cyclopentenol **4** is more stable than **3**, which has large substituents at the same side of the five-membered ring. This is because **3′** was stabilized by a hydrogen bonding-like interaction between one of the hydrogen atoms $H^{\delta+}$ of the phenyl ring and an oxygen atom $O^{\delta-}$ attached to $C_{(H)}$ (see top right figure of Scheme 2 and Fig. 2). Two types of representative geometries (type-A and -B) were obtained by geometry optimizations for many types of conformations in cyclopentenols **3** and **4** using Becke's three-parameter-hybrid (B3LYP) method[18] in density functional theory (DFT) (B3LYP/6-31G(d)) (see Fig. 4). In both cyclopentenols **3** and **4**, the type-A (structure with global minimum energy) is more stable than is the type-B (structure with local minimum energy). In type-A, one of the hydrogen atoms in the phenyl ring directs to an oxygen atom of the hydroxyl group (see the dotted line in Fig. 4). If both **3** and **4** have type-A geometries, cyclopentenol **4** is more stable than **3**. This result agrees with the prediction that **4** would be more stable than **3**. Therefore, we assume that **4′** in Fig. 2 without the hydrogen bonding-like interaction leads to cyclopentenol **4** having type-A geometry after protonation.

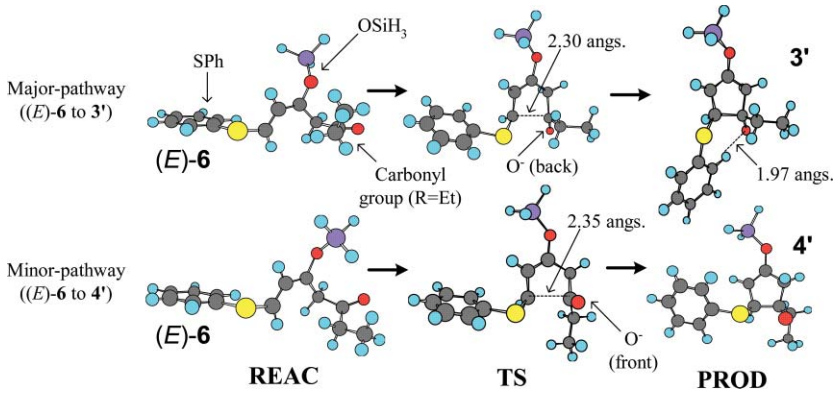

Fig. 2 Optimized geometries in the major ((*E*)-**6** → **3′**) and minor ((*E*)-**6** → **4′**) reaction pathways in the cyclization step (R=Et, HF/6-31G). The **3′** and **4′** correspond to cyclopentenols **3** and **4** before protonation, respectively.

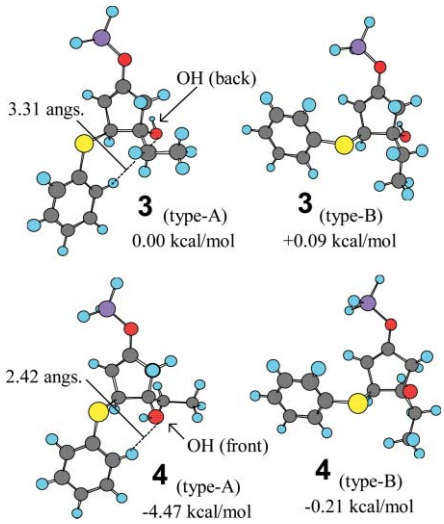

Fig. 4 Two types of optimized geometries for the cyclopentenols **3** and **4** (B3LYP/6-31G(d)). Relative energy (in kcal mol^{-1}) to the total energy of **3** (type-A) is shown below the geometry. In type-A geometry, one of the hydrogen atoms of the phenyl ring is directed toward the oxygen atom of the hydroxyl group (the dotted line indicates the hydrogen bond O···H).

Ab initio through-space/bond interaction analysis on the difference in activation energies of major and minor pathways

What kind of interactions in a molecule causes differences in activation energy between the major and minor pathways? To identify the origin of the difference in activation energy, we applied *ab initio* through-space/bond interaction analysis to this problem at the level of HF/6-31G. Table 1 shows the activation energies $\Delta E^{\ddagger}$ for the cyclization step ((*E*)-**6** → **3**′ and **4**′) after the deletions of various types of through-space interactions related to sulfur (site *A*), silicon (site *F*), oxygen (site *E* and *I*), and carbon (site *B*) atoms. The "diff." indicates the difference of the activation energies between the major and minor pathways, that is, diff. = $\Delta E^{\ddagger}$(major) − $\Delta E^{\ddagger}$(minor). "Full interaction" includes all intramolecular interactions (without any deletions). Small changes of activation energies for the major and minor pathways do not fundamentally change the diff. values in the "delete $S_{(A)}$–$O_{(E)}$", "delete $S_{(A)}$–$Si_{(F)}$", "delete $S_{(A)}$–$O_{(I)}$" and "delete $Si_{(F)}$–$O_{(I)}$" states. In contrast, in the deletions of the interactions related to the carbanion ($C_{(B)}$ atom), it was found that the absolute value of diff. decreases compared with that of "full interaction." This means that the interactions related to the carbanion $C_{(B)}$ causes the difference in activation energy between the major and minor pathways. In the "delete $C_{(B)}$–$Si_{(F)}$" state, in particular, both the major and minor pathways have similar activation energies (diff. = −0.28 kcal mol^{-1}). Table 2 shows more detailed analysis of the interaction $S_{(A)}$–$O_{(I)}$, and the interactions related to the carbanion $C_{(B)}$. In "full interaction," the difference in activation energy $\Delta E^{\ddagger}$ between the major and minor pathways, that is, diff. = $\Delta E^{\ddagger}_{\text{major}} - \Delta E^{\ddagger}_{\text{minor}}$ = −2.48 kcal mol^{-1}, was primarily due to diff. with −2.60 kcal mol^{-1} in TS. In "delete $S_{(A)}$–$O_{(I)}$", the difference in $\Delta E^{\ddagger}$ between the major and minor pathways was not changed largely. This is because that both pathways show the same amount of energy stabilizations in TS. In "delete $C_{(B)}$–$O_{(E)}$", it was found that the lowering of the absolute value of "diff." in $\Delta E^{\ddagger}$ (−2.48 kcal mol^{-1} (full interaction) → −1.47 kcal mol^{-1}) is caused by the destabilization of REAC in the minor pathway. We assumed that the difference in energy change in REAC was due to the difference in the directions of lone pair orbitals of $O_{(E)}$ for the major and minor pathways (see also Fig. 2). The diff. in $\Delta E^{\ddagger}$ with −0.28 kcal mol^{-1} in "Delete $C_{(B)}$–$Si_{(F)}$" and with 0.96 kcal mol^{-1} in "delete $C_{(B)}$–$O_{(I)}$" comes from the large stabilization of the TS in the minor pathway. For example, in "delete $C_{(B)}$–$Si_{(F)}$", the stabilization of the TS (compared with "full interaction") in the minor pathway with −0.00962 a.u. is larger than that in the major pathway with −0.00655 a.u. This means that the TS of the minor-pathway has a larger repulsion $C_{(B)} \leftrightarrow Si_{(F)}$ or $C_{(B)} \leftrightarrow O_{(I)}$ than that of the major pathway in "full interaction." This produces the relative stability of the TS in the major pathway. In "delete $C_{(B)}$–$O_{(I)}$" state, the TS is more stable than REAC for both pathways ($\Delta E^{\ddagger} < 0$) and, thus, the values of "diff." are positive. This result shows that the repulsion between $C_{(B)}^{\delta-}$ and $O_{(I)}^{\delta-}$ in the TS is more effective than that in REAC. Therefore, the difference in such repulsions related to the carbanion $C_{(B)}$ in the TS makes the difference in $\Delta E^{\ddagger}$ between the major and minor pathways.

To examine the contribution of the phenyl ring (in the phenylthio group) on the reaction pathways, we compared the optimized geometries and activation energies for (*E*)-**6** including the –SMe group instead of the –SPh group with (*E*)-**6** at the level of the HF/6-31G basis set. It was found that the –SMe and –SPh models show similar geometries and activation energies in the reaction pathways. In the –SMe model, $\Delta E^{\ddagger}$ was estimated with 13.05 and 15.79 kcal mol^{-1} for the major and minor pathways, respectively. Therefore, it can be concluded that the steric and resonance effects of the phenyl ring are not important for the reaction pathways in question.

Table 1 *Ab initio* through-space/bond interaction analysis for the activation energy $\Delta E^{\ddagger}$ (in kcal mol^{-1}) of the cyclization step (HF/6-31G)

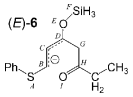

State[a]	Activation energy $\Delta E^{\ddagger}$/kcal mol^{-1}		
	Major pathway ((*E*)-**6** → **3**′)	Minor pathway ((*E*)-**6** → **4**′)	Diff.[b]
Full interaction	13.37	15.85	−2.48
Delete $S_{(A)}$–$O_{(E)}$	13.24	15.63	−2.39
Delete $S_{(A)}$–$Si_{(F)}$	13.27	15.87	−2.60
Delete $S_{(A)}$–$O_{(I)}$	12.81	15.19	−2.37
Delete $C_{(B)}$–$O_{(E)}$	11.74	13.20	−1.47
Delete $C_{(B)}$–$Si_{(F)}$	11.12	11.40	−0.28
Delete $C_{(B)}$–$O_{(I)}$	−2.87	−3.83	0.96
Delete $Si_{(F)}$–$O_{(I)}$	13.50	16.14	−2.64

[a] Outer functions of split valence p-orbitals are deleted. For example, "delete $S_{(A)}$–$O_{(E)}$" indicates the deletion of the interactions between the 3p(outer)-orbitals of the sulfur atom at site *A* and 2p(outer)-orbitals of the oxygen atom at site *E*. Sites *A*–*I* are shown in the top figure. [b] Difference of activation energy $\Delta E^{\ddagger}$ between major and minor pathways, diff. = $\Delta E^{\ddagger}$(major) − $\Delta E^{\ddagger}$(minor).

Ab initio MO approach to the loss of stereochemical integrity in starting materials

Another indeterminate problem is the loss of stereochemical integrity in the starting materials. To examine the change in geometry and electronic structure caused by Brook rearrangement, we performed geometry optimizations for (*E*)-**5** and (*E*)-**6** using both HF and DFT. Bond lengths and Mulliken's net charge of both molecules are listed in Table 3. It was found that all calculations exhibit a similar tendency. The $C_{(B)}$–$C_{(C)}$ length with 1.325–1.342 Å in (*E*)-**5** corresponds to a double bond. Brook rearrangement changed the $C_{(B)}$–$C_{(C)}$–$C_{(D)}$ structure of (*E*)-**5** to a delocalized allylic anion structure in (*E*)-**6**. In particular, the $C_{(B)}$–$C_{(C)}$ length in (*E*)-**6** with 1.410–1.416 Å strongly involves a single bond property compared with the $C_{(B)}$–$C_{(C)}$ length in (*E*)-**5**. Therefore, the $C_{(B)}$–$C_{(C)}$ bond in (*E*)-**6** has a weak C–C single bond nature compared with the $C_{(B)}$–$C_{(D)}$ bond, which is opposite to the case of (*E*)-**5**. In addition, it was found from Mulliken's

Table 2 Through-space/bond interaction analysis (HF/6-31G) of the interaction $S_{(A)}$–$O_{(I)}$ and interactions related to carbanion $C_{(B)}$ in (*E*)-**6** for major ((*E*)-**6** → **3**′) and minor ((*E*)-**6** → **4**′) reaction pathways

State[a]	Pathway	Total energy/a.u. REAC		TS		Activation energy $\Delta E^{\ddagger}$
Full interaction	Major	−1337.96074		−1337.93943		13.37 kcal mol^{-1}
	Minor	−1337.96054		−1337.93529		15.85 kcal mol^{-1}
	Diff.[b]	−0.12 kcal mol^{-1}		−2.60 kcal mol^{-1}		−2.48 kcal mol^{-1}
Delete $S_{(A)}$–$O_{(I)}$	Major	−1337.96072	(+0.00002)[c]	−1337.94031	(−0.00088)	12.81 kcal mol^{-1}
	Minor	−1337.96054	(+0.00000)	−1337.93634	(−0.00105)	15.19 kcal mol^{-1}
	Diff.	−0.11 kcal mol^{-1}		−2.49 kcal mol^{-1}		−2.37 kcal mol^{-1}
Delete $C_{(B)}$–$O_{(E)}$	Major	−1337.96100	(−0.00026)	−1337.94229	(−0.00286)	11.74 kcal mol^{-1}
	Minor	−1337.95951	(+0.00103)	−1337.93847	(−0.00318)	13.20 kcal mol^{-1}
	Diff.	−0.93 kcal mol^{-1}		−2.40 kcal mol^{-1}		−1.47 kcal mol^{-1}
Delete $C_{(B)}$–$Si_{(F)}$	Major	−1337.96370	(+0.00296)	−1337.94598	(−0.00655)	11.12 kcal mol^{-1}
	Minor	−1337.96307	(+0.00253)	−1337.94491	(−0.00962)	11.40 kcal mol^{-1}
	Diff.	−0.40 kcal mol^{-1}		−0.67 kcal mol^{-1}		−0.28 kcal mol^{-1}
Delete $C_{(B)}$–$O_{(I)}$	Major	−1337.96085	(−0.00011)	−1337.96542	(−0.02599)	−2.87 kcal mol^{-1}
	Minor	−1337.96063	(−0.00009)	−1337.96674	(−0.03145)	−3.83 kcal mol^{-1}
	Diff.	−0.13 kcal mol^{-1}		0.83 kcal mol^{-1}		0.96 kcal mol^{-1}

[a] Site symbols *A*, *B*, *E*, *F*, and *I* are shown in the top figure of Table 1. [b] Total energy difference between major and minor reaction pathways, diff. = major − minor (in kcal mol^{-1}). [c] Relative energy to "full interaction" are shown in parentheses (in a.u.).

Table 3 Comparison of bond lengths and Mulliken's net charge in (*E*)-**5** and (*E*)-**6**

Basis set	Bond length/Å Bond[a]	(*E*)-**5**	(*E*)-**6**	Diff.[b]	Mulliken's net charge Site[a]	(*E*)-**5**	(*E*)-**6**	Diff.[c]	[Sum][d]
HF/6-31G	$C_{(C)}$–$C_{(D)}$	1.507	1.355	−0.152	$C_{(C)}$	+0.049	−0.042	−0.091	
	$C_{(B)}$–$C_{(C)}$	1.325	1.410	+0.085	$C_{(B)}$	−0.585	−0.705	−0.120	[−0.211]
B3LYP/6-31G	$C_{(C)}$–$C_{(D)}$	1.520	1.380	−0.140	$C_{(C)}$	+0.050	−0.087	−0.087	
	$C_{(B)}$–$C_{(C)}$	1.341	1.411	+0.070	$C_{(B)}$	−0.456	−0.078	−0.078	[−0.165]
B3LYP/6-31G(d)	$C_{(C)}$–$C_{(D)}$	1.518	1.372	−0.146	$C_{(C)}$	−0.020	−0.095	−0.075	
	$C_{(B)}$–$C_{(C)}$	1.342	1.416	+0.074	$C_{(B)}$	−0.368	−0.451	−0.083	[−0.158]

[a] Refer to site symbols in Scheme 2. [b] Change in bond length (Å), diff. = (*E*)-**6** − (*E*)-**5**. [c] Change in net charge, diff. = (*E*)-**6** − (*E*)-**5**. [d] Total change in net charges, that is, the sum of diff. in $C_{(C)}$ and that in $C_{(B)}$.

net charge that Brook rearrangement causes the delocalization of a negative charge into the $C_{(B)}$ and $C_{(C)}$ atoms.

Rotational barriers for the inversion (*E*)-**6** → (*Z*)-**6** were calculated using the HF/6-31G and HF/6-31G(d) basis sets to examine the possibility of *E*/*Z* inversion in **6**. The results are listed in Table 4. We adopted fully relaxed rotation; that is, all parameters except for the dihedral angle ϕ are optimized for each ϕ. In the result for HF/6-31G, both the barrier heights with +11.08 kcal mol^{-1} (clockwise rotation) and +9.97 kcal mol^{-1} (counterclockwise rotation) are lower than the activation energy of the major pathway with 13.37 kcal mol^{-1}. Similarly, in the result for HF/6-31G(d), both the barrier heights with +10.99 kcal mol^{-1} (clockwise rotation) and with +11.62 kcal mol^{-1} (counterclockwise rotation) are lower than the activation energy of the major pathway with 15.97 kcal mol^{-1}. These results mean that *E*/*Z* inversion preferentially occurs even at low temperatures where the cyclization step would not occur. This result clearly explains the *E*/*Z* isomerization observed in the experiment. In addition, it was found that the energy of (*E*)-**6** was more stable than that of (*Z*)-**6** in both basis sets. The experimental and theoretical results imply that the cyclization step in [3 + 2] annulation is started from the (*E*)-isomer rather than the (*Z*)-isomer because of the difference in the *E*/*Z* distribution.

Table 4 Rotational barrier[a] for *E*/*Z* conformational inversion and energy difference between (*E*)-**6** and (*Z*)-**6**. The model molecule for the *E*/*Z* inversion is shown below the table

Basis set	Barrier for *E*/*Z* inversion (*E*)-**6** to (*Z*)-**6**/kcal mol^{-1} Rotate clockwise	Rotate counterclockwise	Total energy/a.u. (*E*)-**6**	(*Z*)-**6**	Diff.[b](kcal/mol)
HF/6-31G	+11.08	+9.97	−1337.96207	−1337.95878	−2.07
HF/6-31G(d)	+10.99	+11.62	−1338.31813	−1338.31415	−2.50

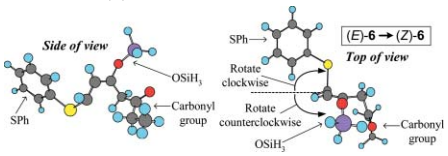

[a] Fully relaxed rotation was adopted. [b] Diff. = E_{total}((*E*)-**6**) − E_{total}((*Z*)-**6**).

Conclusion

In the present article, *ab initio* through-space/bond interaction analysis was performed for the uncertain mechanisms of reaction pathways in [3 + 2] annulation. It was found that the orbital interactions related to the carbanion generated by Brook rearrangement destabilize the minor pathway in the cyclization step by the repulsion to other atoms, which produces the stability of the transition state in the major pathway to a bulky product **3**. This result supports the experiment that demonstrated that the bulky product becomes a majority. In addition, *ab initio* MO calculations clarified that the *E*/*Z* isomerization of the starting material **1** can be explained by an *E*/*Z* conformational inversion between (*E*)-**6** and (*Z*)-**6**. We trust that our conclusions will shed light on the mechanism of [3 + 2] annulation and will contribute to the control of the stereoselective construction of odd-membered carbocycles.

Acknowledgements

This work was supported by a grant-in-aid from the Ministry of Education, Culture, Sports, Science and Technology of Japan (MEXT) and by the Research and Development Applying Advanced Computational Science and Technology of the Japan Science and Technology Agency (ACT-JST). The calculations were performed on systems in our laboratory, including Linux PCs, IBM RISC/6000 and SGI ORIGIN2000.

References

1 M. Ramaiah, *Synthesis*, 1984, 529–570; T. Hudlicky, F. Rulin, T. C. Lovelace and J. W. Reed, in *Studies in Natural Products Chemistry*, ed. T. Attaur-Rahman, Elsevier Science, Essex, UK, 1989, pp. 3–72; T. L. Ho, *Carbocycle Construction in Terpene Synthesis*, VCH, New York, 1988.

2 R. D. Little, in *Comprehensive Organic Synthesis*, ed. B. M. Trost and I. Freming, Pergamon, Oxford, 1991, vol. 5, pp. 239–270; R. L. Danheiser, B. R. Dixon and K. W. Gleason, *J. Org. Chem.*, 1992, **57**, 6094–6097; S. Ejiri, S. Yamago and E. Nakamura, *J. Am. Chem. Soc.*, 1992, **114**, 8707–8708; J. W. Herndon, C. Wu, J. J. Harp and K. A. Kreutzer, *Synlett*, 1991, 1–10.

3 K. Takeda, M. Fujisawa, T. Makino and E. Yoshii, *J. Am. Chem. Soc.*, 1993, **115**, 9351–9352.

4 K. Takeda, *J. Synth. Org. Chem. Jpn.*, 1997, **55**, 774–784.

5 K. Takeda, Y. Ohtani, E. Ando, K. Fujimoto, E. Yoshii and T. Koizumi, *Chem. Lett.*, 1998, 1157–1158.

6 K. Takeda, K. Yamawaki and N. Hatakeyama, *J. Org. Chem.*, 2002, **67**(6), 1786–1794.

7 A. G. Brook, *J. Am. Chem. Soc.*, 1957, **79**, 4373–4375; A. G. Brook, *Acc. Chem. Res.*, 1974, **7**, 77–84; A. G. Brook and A. R. Bassindale, in *Rearrangements in Ground and Excited States*, ed. P. de Mayo, Academic Press, New York, 1980, pp. 149–221; H. J. Reich, R. C. Holtan and C. Bolm, *J. Am. Chem. Soc.*, 1990, **112**, 5609–5617.

8 K. Takeda, I. Nakayama and E. Yoshii, *Synlett*, 1994, 178–178; K. Takeda, K. Kitagawa, I. Nakayama and E. Yoshii, *Synlett*, 1997, 255–256.

9 R. Hoffmann, A. Imamura and W. J. Hehre, *J. Am. Chem. Soc.*, 1968, **90**, 1499–1509.

10 A. J. Post, J. J. Nash, D. E. Love, K. D. Jordan and H. Morrison, *J. Am. Chem. Soc.*, 1995, **117**, 4930–4935; H. Lange, W. Schafer, R. Gleiter, P. Camps and S. Vazquez, *J. Org. Chem.*, 1998, **63**, 3478–3480; V. Gineityte, *J. Mol. Struct.*, 1998, **430**, 97–104; H. Mackenzie-Ross, M. J. Brunger, F. Wang, W. Adcock, N. Trout, I. E. McCarthy and D. A. Winkler, *J. Electron. Spectrosc. Relat. Phenom.*, 2002, **123**, 389–395; S. P. de Visser, M. Filatov, P. R. Schreiner and S. Shaik, *Eur. J. Org. Chem.*, 2003, 4199–4204.

11 A. Imamura, H. Sugiyama, Y. Orimoto and Y. Aoki, *Int. J. Quantum Chem.*, 1999, **74**, 761–768; Y. Orimoto and Y. Aoki, *Int. J. Quantum Chem.*, 2002, **86**, 456–467; Y. Orimoto, K. Naka and Y. Aoki, *Int. J. Quantum Chem.*, 2005, DOI: 10.1002/qua.20614.

12 P. Deslongchamps, *Stereoelectronic effects in organic chemistry*, Pergamon, Oxford, 1993; A. J. Kirby, *Stereoelectronic effects*, Oxford University Press, Oxford, 1996.

13 Y. Orimoto and Y. Aoki, *Int. J. Quantum Chem.*, 2003, **92**, 355–366.

14 Y. Orimoto and Y. Aoki, *Phys. Rev. A: At., Mol., Opt. Phys.*, 2003, **68**, 063808/1-063808/6.

15 GAMESS, M. W. Schmidt, K. K. Baldridge, J. A. Boatz, S. T. Elbert, M. S. Gordon, J. H. Jensen, S. Koseki, N. Matsunaga, K. A. Nguyen, S. J. Su, T. L. Windus, M. Dupuis and J. A. Montgomery, *J. Comput. Chem.*, 1993, **14**, 1347–1363.

16 M. J. Frisch, G. W. Trucks, H. B. Schlegel, G. E. Scuseria, M. A. Robb, J. R. Cheeseman, V. G. Zakrzewski, J. A. Montgomery, Jr., R. E. Stratmann, J. C. Burant, S. Dapprich, J. M. Millam, A. D. Daniels, K. N. Kudin, M. C. Strain, O. Farkas, J. Tomasi, V. Barone, M. Cossi, R. Cammi, B. Mennucci, C. Pomelli, C. Adamo, S. Clifford, J. Ochterski, G. A. Petersson, P. Y. Ayala, Q. Cui, K. Morokuma, P. Salvador, J. J. Dannenberg, D. K. Malick, A. D. Rabuck, K. Raghavachari, J. B. Foresman, J. Cioslowski, J. V. Ortiz, A. G. Baboul, B. B. Stefanov, G. Liu, A. Liashenko, P. Piskorz, I. Komaromi, R. Gomperts, R. L. Martin, D. J. Fox, T. Keith, M. A. Al-Laham, C. Y. Peng, A. Nanayakkara, M. Challacombe, P. M. W. Gill, B. G. Johnson, W. Chen, M. W. Wong, J. L. Andres, C. Gonzalez, M. Head-Gordon, E. S. Replogle and J. A. Pople, *GAUSSIAN 98*, Gaussian, Inc., Pittsburgh, PA, 2001.

17 K. Fukui, *J. Phys. Chem.*, 1970, **74**, 4161–4163; K. Fukui, *Acc. Chem. Res.*, 1981, **14**, 363–368.

18 A. D. Becke, *J. Chem. Phys.*, 1993, **98**, 5648–5652; C. Lee, W. Yang and R. G. Parr, *Phys. Rev. B: Condens. Matter*, 1988, **37**, 785–789; B. Miehlich, A. Savin, H. Stoll and H. Preuss, *Chem. Phys. Lett.*, 1989, **157**, 200–206.